

# A Modified Decoupled Semi-Analytical Approach Based On SBFEM for Solving 2D Elastodynamic Problems

M. Fakharian, M. I. Khodakarami

**Abstract**—In this paper, a new trend for improvement in semi-analytical method based on scale boundaries in order to solve the 2D elastodynamic problems is provided. In this regard, only the boundaries of the problem domain discretization are by specific sub-parametric elements. Mapping functions are uses as a class of higher-order Lagrange polynomials, special shape functions, Gauss-Lobatto-Legendre numerical integration, and the integral form of the weighted residual method, the matrix is diagonal coefficients in the equations of elastodynamic issues. Differences between study conducted and prior research in this paper is in geometry production procedure of the interpolation function and integration of the different is selected. Validity and accuracy of the present method are fully demonstrated through two benchmark problems which are successfully modeled using a few numbers of DOFs. The numerical results agree very well with the analytical solutions and the results from other numerical methods.

**Keywords**—2D Elastodynamic Problems, Lagrange Polynomials, G-L-Quadrature, Decoupled SBFEM.

## I. INTRODUCTION

TO solve elastodynamic problems for analysis and design purposes, numerical approaches are usually employed. Different types of numerical approaches such as Finite Element Method (FEM), Boundary Element Method (BEM), Scaled Boundary Finite Element Method (SBFEM), and meshless methods are routinely used to solve elastodynamic problems. The use of FEM is advantageous as its procedures are well-established and versatile in nature. On the other hand, BEM requires basically reduced surface discretizations, and may be considered as an appealing alternative to FEM for elastodynamic problems. Since BEM does not require domain discretization, fewer unknowns are required to be stored. BEM needs a fundamental solution for the governing differential equation to obtain the boundary integral equation. Although coefficient matrices of BEM are much smaller than those of FEM, they are routinely non-positive definite, non-symmetric, and fully populated. Combining the advantages of FEM and BEM, SBFEM was successfully developed. Using surface finite elements, SBFEM discretizes only the boundary of the domain by transforming the governing partial differential equations to ordinary differential equations, which may be

solved analytically. SBFEM, which requires no fundamental solution, have also been employed for the analysis of elastodynamic problems [1]. A modification of the SBFEM with Diagonal coefficient matrices has been proposed in [2] for solving potential problems and it is applied to solve elastostatic problems [3], also the proposed method is used to solve elastodynamic problems in [4], moreover it is also the method to solve the three-dimensional elastostatic problems [5] and an infinite half-space problems is used[6].

In this study, we improved the efficiency of the semi-analytical approach which is proposed in [4]; where, the Lagrange polynomials is used as mapping functions instead of Chebyshev polynomials and also Gauss-Lobatto-Legendre quadrature is employed instead of Clenshaw-Curtis integration technique in order to calculate the coefficient matrices. By the way, with implementing this technique, the governing equations for each node are independent of the other nodes and this will reduce the computational costs. Accuracy of the present method is demonstrated through two benchmark problems and its results are shown a good agreement between this approach and other methods.

## II. GOVERNING EQUATIONS

The governing equilibrium equations for elastodynamic problems may be solved based upon either a strong or a weak formulation of the problem. In the strong formulation, one may directly deal with the equilibrium equations of the problem and associated boundary conditions written in a differential form. In the weak formulation on the other hand, one may use an integral form of the equilibrium equations.

The present new method is based on a weak formulation of the governing equations of elastodynamic problems. The equilibrium equations for a two-dimensional bounded medium  $\Omega$  is described by

$$\sigma_{ij,j} + f_i = \rho \ddot{u}_i \quad (1)$$

in which  $\sigma_{ij}$  indicates the stress tensor components. In addition,  $f_i$  denotes the external source of exciting forces generated per unit volume, respectively,  $\ddot{u}_i = \partial^2 u_i / \partial t^2$  and  $\rho$  is the mass density. For a 2D problem in global Cartesian coordinates,  $i = X, Y$  and  $j = X, Y$  (see Fig. 1). Instead of using the governing equations and associated boundary conditions directly, strong form as in (1), one may use an integrated. This may be accomplished by weighting (1) with an arbitrary

M. Fakharian is with the Faculty of Civil Engineering, Semnan University, Semnan, Iran (e-mail:majid.fakharian.21@gmail.com).

M. I. Khodakarami is with the Faculty of Civil Engineering, Semnan University, Semnan, Iran (corresponding author to provide phone: (98) 23-3338-3774; fax:(98)23-3336-5421; e-mail:khodakarami@profs.semnan.ac.ir).

weighting function ( $w$ ), and integrating over the problem domain  $\Omega$  and applying the boundary conditions. The result may be given by

$$\int_{\Omega} w(\sigma_{ij,j} + f_{ii} - \rho \ddot{u}_i) d\Omega = 0 \quad (2)$$

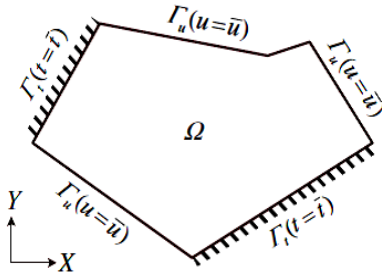


Fig. 1 A 2D domain ( $\Omega$ ) with Dirichlet ( $\Gamma_u$ ) and Neumann ( $\Gamma_t$ ) boundary conditions for elastodynamic problems

### III. GEOMETRY MODELING

In the present method, for a bounded medium, a local-coordinates-origin (LCO) is chosen from which all boundaries of the domain are visible (Fig. 2). For bounded domains of this research, the LCO is selected inside the domain or on the boundary. Consequently, the total boundary of the domain includes two regions: the region that pass through the LCO (such as  $\Gamma_1$  and  $\Gamma_5$  in Fig. 2 (a)), and the other remaining region. In the present method, only the region that does not pass through the LCO should be decomposed into  $n_e$  one-dimensional non-isoparametric elements  $\Gamma_e$ ,  $e = 1, 2, \dots, n_e$ , so that  $\Gamma = \cup_{e=1}^{n_e} \Gamma_e$ .

In this method, a geometry transmission is introduced from global Cartesian coordinates ( $\hat{x}, \hat{y}$ ) to local dimensionless coordinates ( $\xi, \eta$ ) (see Fig. 2). This transmission is obtained by Lagrange polynomials as mapping functions. Two local coordinates are defined as  $\xi$  is radial coordinate from the LCO to the boundaries and  $\eta$  is tangential coordinate on the boundaries. The radial coordinate  $\xi$  is equal to zero at the LCO and is equal to 1 on the boundaries. The tangential coordinate  $\eta$  varies between -1 and +1 on the boundaries.

In addition, displacement and stress of each node are interpolated by special shape functions that are introduced in this paper. Mapping functions and the special shape functions are illustrated in following sections.

Each element on the boundary is analogous to a line; so, we adopt an appropriate mapping between the line (reference/master element) and each element  $\Gamma_e$ . In the present method, sub-parametric elements are proposed. Each element  $\Gamma_e$  is defined in terms of a set of mapping functions  $\Phi_i(\eta)$ ,  $i = 1, 2, \dots, n_\eta + 1$ . The geometry of elements in local coordinates is then given as

$$\{x(\eta)\} = [\Phi(\eta)] \{x\} \quad (3)$$

where,  $\{x(\eta)\}$  denote the vector of global coordinates of boundary points; and any point in the domain with  $\{\hat{x}\}$  coordinates relates to the corresponding point on the elements of boundary as

$$\{\hat{x}(\xi, \eta)\} = \xi \{x(\eta)\} \quad (4)$$

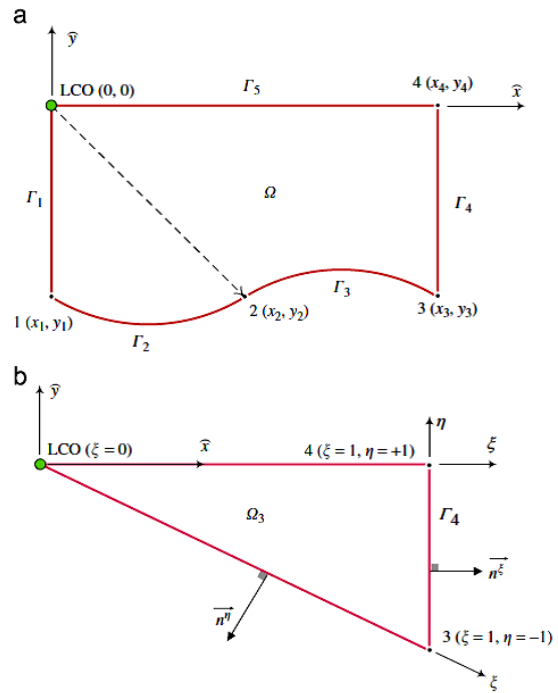


Fig. 2 Modeling of 2D bounded domain, and the LCO: (a) in global coordinates system, and (b) in scaled boundary local system

The proposed mapping functions for an  $(n_\eta + 1)$ -node element is introduced as [7]:

$$\varphi_i = \prod_{k=1, k \neq i}^{n_\eta+1} \frac{\eta - \eta_k}{\eta_i - \eta_k} \quad (5)$$

Considering (5), the Lagrange polynomials have the properties of the Kronecker Delta at any G-L-L node of the elements on the boundaries. To this end, let's consider a differential element of area  $d\hat{x}d\hat{y}$  which is related to a differential element of area  $d\xi d\eta$  by

$$d\Omega = d\hat{x}d\hat{y} = |\hat{J}(\xi, \eta)| d\xi d\eta = \xi |J(\eta)| d\xi d\eta \quad (6)$$

where,  $\hat{J}(\xi, \eta)$  indicates the  $2 \times 2$  Jacobian matrix of the transformation, and is evaluated as:

$$\hat{J}(\xi, \eta) = \begin{vmatrix} \frac{\partial \hat{x}}{\partial \xi} & \frac{\partial \hat{x}}{\partial \eta} \\ \frac{\partial \hat{y}}{\partial \xi} & \frac{\partial \hat{y}}{\partial \eta} \end{vmatrix}; \quad \hat{x} = \begin{Bmatrix} \hat{x} \\ \hat{y} \end{Bmatrix} \quad (7)$$

On the boundary, the Jacobian matrix may be written in the following form:

$$J(\eta) = \begin{bmatrix} x(\eta) & y(\eta) \\ x_{,\eta}(\eta) & y_{,\eta}(\eta) \end{bmatrix} \quad (8)$$

The spatial derivatives of a virtual vector  $\{S\} = [S_{\bar{x}} S_{\bar{y}}]^T$  in global coordinates system are defined in terms of the virtual vector by the well-known relation that defines the operator  $[L]$

$$\begin{Bmatrix} S_{,\bar{x}} \\ S_{,\bar{y}} \\ S_{,\bar{x}} + S_{,\bar{y}} \end{Bmatrix} = \begin{bmatrix} \frac{\partial}{\partial \bar{x}} & 0 & \frac{\partial}{\partial \bar{y}} \\ 0 & \frac{\partial}{\partial \bar{y}} & \frac{\partial}{\partial \bar{x}} \end{bmatrix}^T \begin{Bmatrix} S_{\bar{x}} \\ S_{\bar{y}} \end{Bmatrix} \quad (9)$$

The spatial derivatives in the two coordinate systems are related as

$$\begin{bmatrix} \frac{\partial}{\partial \bar{x}} & 0 & \frac{\partial}{\partial \bar{y}} \\ 0 & \frac{\partial}{\partial \bar{y}} & \frac{\partial}{\partial \bar{x}} \end{bmatrix}^T = [b^1(\eta)] \frac{\partial}{\partial \xi} + [b^2(\eta)] \frac{1}{\xi} \frac{\partial}{\partial \eta} \quad (10)$$

where,

$$[b^1(\eta)] = \frac{1}{|J(\eta)|} \begin{bmatrix} y(\eta)_{,\eta} & 0 \\ 0 & -x(\eta)_{,\eta} \\ -x(\eta)_{,\eta} & y(\eta)_{,\eta} \end{bmatrix} \quad (11)$$

$$[b^2(\eta)] = \frac{1}{|J(\eta)|} \begin{bmatrix} -y(\eta) & 0 \\ 0 & x(\eta) \\ x(\eta) & -y(\eta) \end{bmatrix} \quad (12)$$

#### IV. SHAPE FUNCTIONS

In this method, special polynomials  $N(\eta)$  are used as shape functions, diagonal coefficient matrices will be derived by using these shape functions for solving problems. To this end, the displacement function and its derivatives, across the element, are interpolated using polynomials that own two specific characteristics; the shape functions have Kronecker Delta property, and their first derivatives are equal to zero at any given control point.

For an element with  $(n_\eta+1)$  nodes, these shape functions are expressed as a polynomial of degree  $(2n_\eta+1)$  as [3]:

$$N_i(\eta) = \sum_{m=0}^{2n_\eta-1} a_m \eta^m \quad (13)$$

The displacement field  $\{u(\xi, \eta, t)\}$  at any point  $(\xi, \eta)$  and time  $t$  is obtained by interpolation of the displacement function using shape functions. For a two dimensional problem, the displacement field may be written in the following form:

$$\{u(\xi, \eta, t)\} = [N(\eta)] [u_x(\xi, t) \quad u_y(\xi, t)]^T \quad (14)$$

using (10) and (14), the strain vector at a given point  $(\xi, \eta)$  at time  $t$  will be obtained by:

$$\{\varepsilon(\xi, \eta, t)\} = [B^1(\eta)] \{u(\xi, t)\}_{,\xi} + \frac{1}{\xi} [B^2(\eta)] \{u(\xi, \eta)\} \quad (15)$$

where,  $[B^1(\eta)] = [b^1(\eta)] [N(\eta)]$  and  $[B^2(\eta)] = [b^2(\eta)] [N(\eta)]_{,\eta}$ .

As the first derivatives of the shape functions at nodes are zero, the second term of (15) at the G-L-L nodes will be vanished. The relation between strain and stress may be expressed using Hook's Law and (15) using the elasticity matrix  $[D]$  as given by

$$\{\sigma(\xi, \eta, t)\} = [D] ([B^1(\eta)] \{u(\xi, t)\}_{,\xi} + \frac{1}{\xi} [B^2(\eta)] \{u(\xi, \eta)\}) \quad (16)$$

#### V. GOVERNING EQUATIONS SYSTEM

As mentioned before, the weak form of governing equations of elastodynamic problems in global coordinates is expressed as (2). Implementing (10), (16) into (2), leads to

$$[D^0] \{u(\xi, t)\}_{,\xi\xi} \xi + [D^1] \{u(\xi, t)\}_{,\xi} + \xi \{F^b(\xi, t)\} = \xi [M] \{u(\xi, t)\}_{,\eta\eta} \quad (17)$$

where,

$$[D^0] = \int_{-1}^{+1} [B^1(\eta)]^T [D] [B^1(\eta)] |J(\eta)| d\eta \quad (18)$$

$$[D^1] = \int_{-1}^{+1} [B^1(\eta)]_{,\eta}^T [D] [B^2(\eta)] |J(\eta)| d\eta \quad (19)$$

$$[M] = \int_{-1}^{+1} [N(\eta)]^T \rho [N(\eta)] |J(\eta)| d\eta \quad (20)$$

$$\{F^b(\xi, t)\} = \int_{-1}^{+1} [N(\eta)]^T \{f^b(\xi, \eta, t)\} |J(\eta)| d\eta \quad (21)$$

Equation (17) is the system of partial differential equations of radial coordinate  $\xi$  and time  $t$  which represents the governing equation of the present method for elastodynamic problems.

#### VI. NUMERICAL INTEGRATION

In this study, to calculate the vectors and matrices in (17), the Gauss-Lobatto-Legendre numerical integration method is applied. The numerical integration method, calculates the values of the coefficients matrix in the GLL, according to the node element that corresponds to the points and also features a shape functions used, resulting diagonal matrix of coefficients used in the equation. Weight coefficients used in the method of integration is calculated using [7]:

$$w_i = \frac{2}{n(n+1)(n_\eta(\eta_i))^2} \quad (22)$$

Consequently, the components of coefficient matrices may be expressed as:

$$D_{ij}^0 = \delta_{ij} w_i [b^1(\eta_i)]^T [D] [b^1(\eta_i)] |J(\eta_i)| \quad (23)$$

$$D_{ij}^1 = \delta_{ij} w_i [b^1(\eta_i)]_{,\eta}^T [D][b^2(\eta_i)] |J(\eta_i)| \quad (24)$$

$$M_{ij} = \delta_{ij} w_i [N(\eta_i)]^T \rho [N^2(\eta_i)] |J(\eta_i)| \quad (25)$$

where,  $\delta_{ij}$  denotes the Kronecker Delta which results in diagonal coefficient matrices. Consequently, the set of differential equation (17) may be expressed as a single differential equation regarding to a specified point  $i$  as the following expression

$$D_{ii}^0 u(\xi, t)_{i,\xi\xi} \xi + D_{ii}^1 u(\xi, t)_{i,\xi} + \xi F_i^b(\xi, t) = \xi M_{ii} u(\xi, t)_{i,\xi\xi} \quad (26)$$

It is worth while remarking that (26) offers a set of ordinary differential equations for an elastodynamic problem with  $2n$  DOFs. Each differential equation in (26) depends only on the elastodynamic function of the  $i$ th DOF. This means that the coupled system of differential equations has been transformed into decoupled differential equations using a special set of weak formulation procedure, mapping functions, quadrature, and shape functions. In other words, to evaluate the displacement function and its derivatives at a given point, the governing equation that is corresponding to the point should be solved, only. As may be illustrated later, the decoupled differential equations system proposed in this paper may also provide higher rates of convergence by employing a few numbers of DOFs compared to other numerical methods.

#### VII. GENERAL SOLUTION OF THE DECOUPLED EQUATIONS

There are many procedures available in the literature for solving (26), among which Fourier transform technique along with the separation of variables could be employed as adopted in this research. For the  $i$ th DOF, the solution of (26) is assumed as the following form

$$u_i(\xi, t) = \chi_i(\xi) T_i(t) \quad (27)$$

where  $\chi_i(\xi)$  and  $T_i(t)$  are functions of radial direction ( $\xi$ ) and time ( $t$ ), respectively. At first,  $\chi_i(\xi)$  may be determined by solving the homogenous form of partial differential (26) as

$$\xi D_{ii}^0 \chi_i''(\xi) T_i(t) + D_{ii}^1 \chi_i'(\xi) T_i(t) - \xi M_{ii} \chi_i(\xi) \ddot{T}_i(t) = 0, \quad (28)$$

and,

$$M_{ii} \ddot{T}_i(t) = \omega_i^2 T_i(t) \quad (29)$$

In which  $\omega_i$  is the eigenvalue of the  $i$ th DOF. The Fourier transform of (26) using the convolution technique is written as

$$\mathbf{F} \left\{ D_{ii}^0 u(\xi, t)_{i,\xi\xi} * \xi \right\} + \mathbf{F} \left\{ D_{ii}^1 u(\xi, t)_{i,\xi} \right\} - \mathbf{F} \left\{ \xi * M_{ii} u(\xi, t)_{i,\xi\xi} \right\} + \mathbf{F} \left\{ \xi * F_i^b(\xi, t) \right\} = 0 \quad (30)$$

where,  $\mathbf{F}$  denotes the Fourier transform sign, and  $*$  represents the convolution sign. Now, (30) may be rewritten as

$$-D_{ii}^0 \omega_i^2 v(\omega_i, t) \mathbf{F} \{ \xi \} + \frac{I}{\sqrt{2\pi}} D_{ii}^1 \omega_i v(\omega_i, t) - M_{ii} v(\omega_i, t) \mathbf{F} \{ \xi \} + \mathbf{F} \{ F_i^s F_i^b(\xi, t) \} \mathbf{F} \{ \xi \} = 0 \quad (31)$$

in which  $v(\omega_i, t)$  indicates the Fourier transform of  $u(\xi, t)_i$  with respect to  $\xi$ , and  $I$  represents  $\sqrt{-1}$ . Moreover,

$$\mathbf{F} \{ \xi \} = \frac{(-e^{I\omega_i} + I\omega_i + 1)e^{-I\omega_i}}{\omega_i^2 \sqrt{2\pi}} \quad (32)$$

As there are many eigen values obtained by solving the ordinary differential (31) using related boundary conditions, the general solution of the governing partial differential equation will be represented as

$$u_i(\xi, t) = \sum_{n_{\omega}=1}^{\infty} \chi_{in_{\omega}}(\xi) T_{in_{\omega}}(t) \quad (33)$$

where,  $N_{\omega}$  represents the number of eigenvalues considered in each analysis. The proposed method obviously is a semi-analytical solution, which represents approximate numerical solutions on the boundaries, while offering exact analytical solutions within the undertaken domain of the problem.

#### VIII. NUMERICAL EXAMPLES

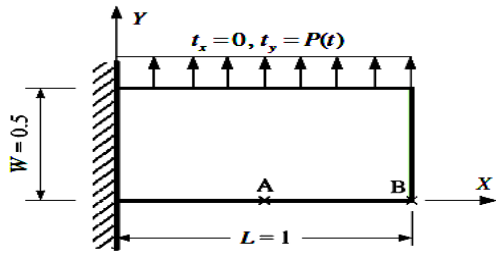
The efficiency and accuracy of the proposed new method is demonstrated through representative numerical examples. To this end, a couple of 2D elastodynamic problems are solved in this section. The results obtained from present method are compared with those reported by other numerical methods and/or exact analytical solutions. All quantities are measured in SI units.

##### A. Cantilever Plate under Transverse Triangular Loading

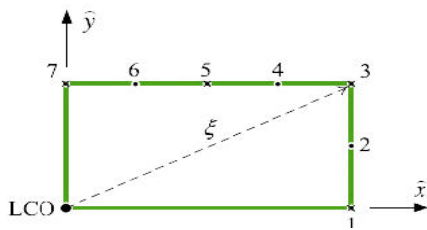
The first example, 2D wave propagation problem is investigated to verify the proposed method in comparison with other numerical solutions. A cantilever plate, shown in Fig. 3 (a), is under a uniform dynamic traction on its upper side. The triangular function of loading increases from zero at time  $t = 0$  to  $P_0$  at  $t = 3$ , and then decreases to zero at  $t = 6$  as depicted in Fig. 3 (c). The material constants are as follows: the Young's modulus  $E=1$ , the mass density  $\rho = 1$  and Poisson's ratio  $\nu = 0.3$ . To model this problem using the proposed method, the LCO is selected as shown in Fig. 3 (b). Moreover, the domain boundary of the problem is discretized using 3 three-node elements with only 7 nodes (see Fig. 3 (b)).

In order to evaluate the histories of vertical displacement at point B, and horizontal stress at point A, the governing equation of node 7 (Fig. 3 (b)) should be solved first. Since the displacement and traction components at the LCO are unique and applicable for all nodes of the domain, after determining

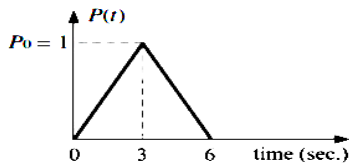
the horizontal and vertical tractions at the LCO, the governing equation of node 1 is solved. Fig. 4 depicts the vertical displacement variations at point B and the horizontal stress variations at point A, due to the transverse triangular loading.



(a)

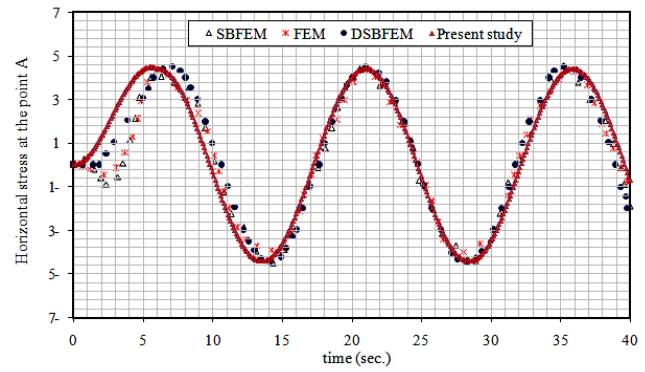


(b)



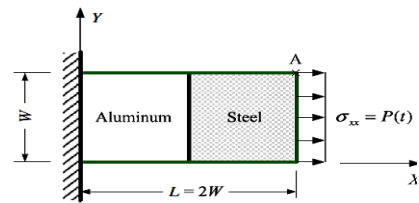
(c)

Fig. 3 2D plane stress plate; (a) geometry and boundary conditions in global Cartesian coordinates, (b) the LCO and the meshes in local coordinates system, (c) time-history of the dynamic loading

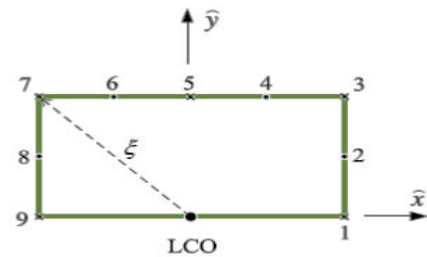


(b)

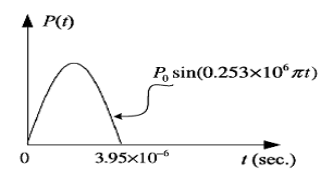
Fig. 4 Results for the first example: (a) Vertical displacement at point B, (b) horizontal stress at point



(a)



(b)



(c)

Fig. 5 Bi-material rectangular plate; (a) geometry and boundary conditions in global Cartesian coordinates, (b) the LCO and the meshing in local coordinates system, (c) sinusoidal dynamic loading

### B. Bi-Material Rectangular Plate Subjected to Impulsive Loading

In order to check the accuracy and efficiency of the present method in the analysis of impact problems, a rectangular plate consisting of two different materials (one half is steel and the other is aluminum) loaded by a sinusoidal impulsive loading (Fig. 5), is studied in the second example. The same geometry and loading function as in are used in this example as:  $L=50\text{mm}$ ,  $P_0 = 100 \text{ MPa}$ . The material properties are: steel Young's modulus  $E_1 = 200 \text{ GPa}$ , aluminum Young's modulus

$E_2 = 70 \text{ GPa}$ ,  $\rho_1 = 7860 \text{ kg/m}^3$ ,  $\rho_2 = 2710 \text{ kg/m}^3$ , and the poisson's ratio of both parts is assumed null ( $\nu_1 = \nu_2 = 0$ ) to impose 1D condition. The LCO is selected at the bottom of materials interface as illustrated in Fig. 5 (b). The corresponding boundaries are discretized employing 4 three-node elements with only 9 nodes.

The time histories of horizontal displacement at point A calculated by the present method are shown in Fig. 6, in which other numerical and analytical solutions are also presented for comparison. Moreover, the time histories of the error distributions in the present method are depicted in this figure.

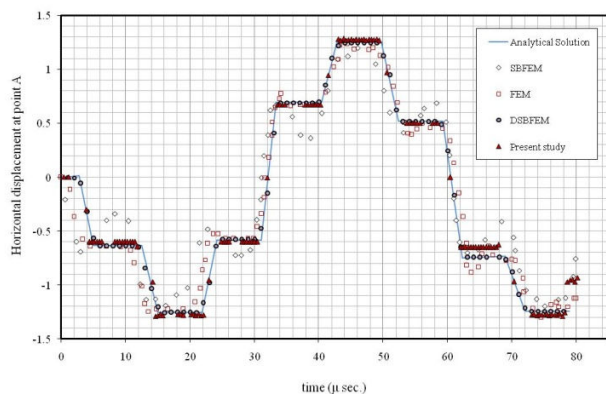


Fig. 6 The variations of horizontal displacement at point A under the sinusoidal loading for the second example

### IX. CONCLUSION

In this research, a new semi-analytical method with its detailed formulation for the analysis of 2D elastodynamic problems was presented. In the proposed method, the boundary of the domain was discretized by new sub-parametric elements with Lagrange polynomials as mapping functions. In addition, these new elements employ new special shape functions formulated to provide Kronecker Delta property for the displacement function and its derivatives. Moreover, the first derivative of shape functions were equated to zero at any given control point. Finally, using Gauss-Lobatto-Legendre quadrature, the coefficient matrices of equations system became diagonal, which leads to a system of decoupled governing equations for the whole system. Analysis of two examples was successfully carried out using the new proposed method. In these examples, various elastodynamic problems and boundary conditions were selected to describe the generality and applicability of the method. It is remarkable that all the examples were successfully modeled with very small number of DOFs, preserving very high accuracy comparing with available analytical and numerical solutions.

### REFERENCES

[1] J.P. Wolf, *The scaled boundary finite element method*. John Wiley & Sons Ltd., 2004.  
 [2] N.Khaji, M.I.Khodakarami, "A new semi-analytical method with diagonal coefficient matrices for potential problems," vol. 35(6), pp. 845-854, Jun. 2011.

[3] M.I. Khodakarami, N.Khaji, "Analysis of elastostatic problems using a semi-analytical method with diagonal coefficient matrices," *Engineering Analysis with Boundary Elements*, vol. 35, pp. 1288-1296, Dec. 2011.  
 [4] M.I. Khodakarami, N. Khaji, M.T. Ahmadi, "Modeling transient elastodynamic problems using a novel semi-analytical method yielding decoupled partial differential equations," *Comput. Methods Appl. Mech. Engrg.*, vol. 213-216, pp. 183-195, Nov. 2012.  
 [5] N. Khaji, M.I. Khodakarami, "A semi-analytical method with a system of decoupled ordinary differential equations for three-dimensional elastostatic problems," *International Journal of Solids and Structures*, vol. 49, pp.2528-2546, Sep. 2012.  
 [6] M.I. Khodakarami, N. Khaji, "Wave propagation in semi-infinite media with topographical irregularities using Decoupled Equations Method," *Soil Dynamics and Earthquake Engineering*, vol. 65, pp.102-112, Oct. 2014.  
 [7] C. Canuto, M.Y. Hussaini, A. Quarteroni, T.A. Zeng, *Spectral Methods in Fluid Dynamics*. Berlin : Springer, 1988.